

## A Model of Calcium Activation of the Cardiac Thin Filament

Edward P. Manning,<sup>†</sup> Jil C. Tardiff,<sup>†</sup> and Steven D. Schwartz\*,<sup>†,‡,§</sup>

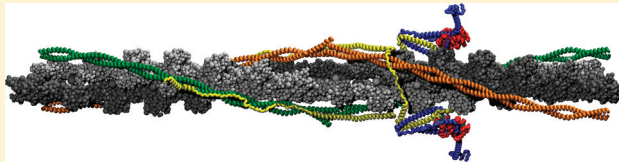
<sup>†</sup>Department of Biophysics, Albert Einstein College of Medicine, 1300 Morris Park Avenue, Bronx, New York 10461, United States

<sup>‡</sup>Department of Biochemistry, Albert Einstein College of Medicine, 1300 Morris Park Avenue, Bronx, New York 10461, United States

<sup>§</sup>Institut des Hautes Études Scientifiques, 91440 Bures-sur-Yvette, France

### Supporting Information

**ABSTRACT:** The cardiac thin filament regulates actomyosin interactions through calcium-dependent alterations in the dynamics of cardiac troponin and tropomyosin. Over the past several decades, many details of the structure and function of the cardiac thin filament and its components have been elucidated. We propose a dynamic, complete model of the thin filament that encompasses known structures of cardiac troponin, tropomyosin, and actin and show that it is able to capture key experimental findings. By performing molecular dynamics simulations under two conditions, one with calcium bound and the other without calcium bound to site II of cardiac troponin C (cTnC), we found that subtle changes in structure and protein contacts within cardiac troponin resulted in sweeping changes throughout the complex that alter tropomyosin (Tm) dynamics and cardiac troponin–actin interactions. Significant calcium-dependent changes in dynamics occur throughout the cardiac troponin complex, resulting from the combination of the following: structural changes in the N-lobe of cTnC at and adjacent to sites I and II and the link between them; secondary structural changes of the cardiac troponin I (cTnI) switch peptide, of the mobile domain, and in the vicinity of residue 25 of the N-terminus; secondary structural changes in the cardiac troponin T (cTnT) linker and Tm-binding regions; and small changes in cTnC–cTnI and cTnT–Tm contacts. As a result of these changes, we observe large changes in the dynamics of the following regions: the N-lobe of cTnC, the mobile domain of cTnI, the I-T arm, the cTnT linker, and overlapping Tm. Our model demonstrates a comprehensive mechanism for calcium activation of the cardiac thin filament consistent with previous, independent experimental findings. This model provides a valuable tool for research into the normal physiology of cardiac myofilaments and a template for studying cardiac thin filament mutations that cause human cardiomyopathies.



The  $\text{Ca}^{2+}$ -based control of cardiac muscle function has long been known to reside in the thin filament. A molecular level understanding of this control, both in health and in disease, is not fully available. This work presents a fully atomistic model of the cardiac troponin (cTn) complex in interaction with tropomyosin (Tm). This model represents the culmination of our efforts<sup>1,2</sup> to apply molecular dynamics simulations to clarify, on a molecular level, the function of the thin filament. The question we are addressing is whether a complete, dynamic model of the thin filament that captures both known structural elements and experimental findings can be constructed. If so, we believe it will (1) assist in describing how various, isolated findings can coexist, (2) reveal new details involving thin filament activation, and (3) provide a useful tool for investigators.

Calcium activation of the thin filament results from cTn's allosteric regulation of Tm dynamics on actin.<sup>3,4</sup> cTn is a complex consisting of three subunits, each of which interacts with the other two. Cardiac troponin C (cTnC) is the site of  $\text{Ca}^{2+}$ -specific binding at site II in the N-lobe of cTnC. Cardiac troponin I (cTnI), the inhibitory subunit, is responsible for inhibition of actomyosin ATPase activity via its interactions with actin<sup>3–5</sup> and forming key intersubunit interactions,

including the formation of a stable coiled coil with cTnT.<sup>6,7</sup> Cardiac troponin T (cTnT) is a link between the calcium-binding core region of cTn and Tm. From structural and biochemical evidence, cTnT–Tm interactions are likely a key step in  $\text{Ca}^{2+}$  signaling propagation between cTn and Tm.<sup>7–9</sup>

The cTn complex can be divided into two regions: a rather stationary globular core domain consisting of portions of cTnC, cTnI, and cTnT<sup>10</sup> and two highly variable regions consisting of the region of cTnT that interacts with Tm and the mobile domain of cTnI that interacts with actin.<sup>7</sup> The flexibility of various regions throughout cTn appears to be fine-tuned, making them sensitive to mutations.<sup>1,2</sup> We hypothesize cTn is also finely tuned to propagate changes in dynamics as a result of  $\text{Ca}^{2+}$  binding.

Tm, a long, flexible coiled coil that bends anisotropically,<sup>11</sup> is in equilibrium among three states of myosin–actin–troponin binding: blocked ( $\text{Ca}^{2+}$  not bound to troponin C, myosin not bound to actin), closed ( $\text{Ca}^{2+}$  bound to troponin C, myosin weakly bound to actin), and open ( $\text{Ca}^{2+}$  bound to troponin C,

**Received:** April 4, 2011

**Revised:** June 28, 2011

**Published:** July 28, 2011

myosin strongly bound to actin).<sup>12,13</sup> Only when Tm is in the open state does one observe actomyosin ATPase activity necessary for force generation of the actin–myosin cross-bridge.<sup>13,14</sup> Ca<sup>2+</sup> binding to cTnC alone is necessary but not fully sufficient to explain Ca<sup>2+</sup> activation of the thin filament.<sup>15</sup> A Ca<sup>2+</sup>-induced signal must propagate through the cTn complex, beginning with Ca<sup>2+</sup> binding in cTnC and ending with cTnT's interactions with Tm, for cTn to regulate Ca<sup>2+</sup> activation of the thin filament. The atomic level mechanism of this propagation remains obscure and, at present, is not accessible via experiment alone.

It was the ability to study the subtle structural and dynamic effects of mutation of this system, along with the possibility of obtaining an atomic level understanding of the function of the thin filament, that motivated this work. For the investigation of the Ca<sup>2+</sup>-based regulation of cardiac tissue, a complete model of cTn is necessary. We have constructed a complete, dynamic, atomistic model of cTn in conjunction with overlapping Tm to simulate cTn in two states: Ca<sup>2+</sup> bound (Ca<sup>2+</sup>-saturated) and Ca<sup>2+</sup> not bound (Ca<sup>2+</sup>-depleted) to site II of the N-lobe of cTnC. This model, the validation presented herein, and its application to calcium control of the cardiac sarcomere are parts of our long-term goal of an integrated computational and experimental elucidation of the mechanisms of thin filament regulation and disease-causing thin filament mutations in cardiac tissue.

We demonstrate that it is possible to construct a dynamic, atomistic model of the entire cTn complex at all temperatures. With this model, we find significant changes in dynamics throughout the cTn subunits as a result of Ca<sup>2+</sup> binding to site II of cTnC, representing equilibrium states of the closed state and a position between the closed and blocked states. We also show that these alterations in cTn dynamics effectively propagate through the cTn complex, resulting in changes to the dynamics of the overlapping region of Tm. Our goal is to make this work accessible to the widest range of biochemists and in particular people beyond the pure simulation community. For this reason, we have elected to put much of the numerical detail in the Supporting Information.

## METHODS

We constructed a thin filament consisting of cTn and overlapping Tm in the closed state oriented to an actin backbone by synthesizing numerous existing atomistic models, including an atomistic model of the cTn core complex from Protein Data Bank (PDB) entry 1J1E,<sup>7</sup> an atomistic model of Tm based on the Lorenz–Holmes model,<sup>16,17</sup> an overlapping model of Tm based on PDB entry 2ZSI,<sup>9</sup> cTnT–Tm interactions based on PDB entry 2ZSH,<sup>9</sup> and an atomistic model of the thin filament including actin, nonoverlapping Tm, and the cTn core.<sup>10</sup> Missing regions of cTn were constructed using secondary structure prediction (PSIPRED)<sup>18,19</sup> and homology with chicken fsTn.<sup>20</sup> The biochemical stoichiometry of the thin filament 7:1:1 (actin:Tm:cTn) may be more accurately described in this case as 14:2:1, where one cTn requires two overlapping Tm's to properly bind, thus requiring 14 actin monomers and two Tm's per cTn. Figure 1 shows our model. Fourteen actin monomers colored silver are associated with the two green overlapping Tm's linked to the top cTn. The second set of 14 actin monomers colored dark gray in Figure 1 is associated with the orange overlapping Tm linked to

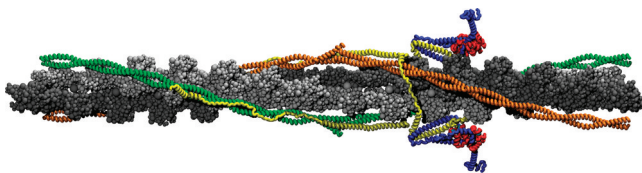


**Figure 1.** Representation of the human thin filament containing human cTn, Tm, and actin: yellow for cTnT, blue for cTnI, red for cTnC, cyan for calcium ion, green/orange for overlapping Tm, and silver/gray for actin filament (the same color scheme is used in the provided movies, except calcium ions in the movie are colored black vice cyan). This figure was obtained by orienting the cTn and Tm to an actin backbone, docking cTnT to overlapping Tm, and performing a 50 ps simulation in equilibrium at 70 K using CHARMM version 33b1<sup>23</sup> of cTn and the overlapping Tm without actin. The resulting cTn–Tm complex is shown here in duplicate with actin added.

the bottom cTn. A schematic of the detailed method by which we built our model is diagrammed in Figure 2.

The thin filament was constructed in the closed state by fixing nonoverlapping tropomysin in the closed positions on actin while cTn and overlapping tropomyosin were allowed to move freely. Two cTn atoms were held in place with harmonic constraints of 2 kcal mol<sup>-1</sup> Å<sup>-1</sup> to anchor cTn over actin (see sections 1–10 of the Supporting Information).

In the construction of our model, we used 629 pertinent “known” interactions of cTn, Tm, and the cTn–Tm complex. This includes 620 protein–protein interactions and nine water bridge interactions based on PDB entries 1J1E, 2ZSH, and 2ZSI<sup>21</sup> (see Protein–protein interactions of the Supporting Information). These atom–atom interactions were simulated using NOE constraints in CHARMM version 33b1 but were relaxed to zero as the model stabilized.<sup>22,23</sup> NOE constraints are designed to introduce a distance restraint between two atoms, using harmonic forces to guide the system toward an optimal equilibrium state. In this case, the optimal equilibrium state was expected to satisfy the structural conditions provided by PDB entries 1J1E, 2ZSI, and 2ZSH without NOE constraints in place, which was successfully accomplished. The total cTn–Tm–Tm complex consists of 28847 atoms, including 1781 residues, four waters, and three calcium ions.

An initial simulation was performed to finalize the building of our model, specifically to dock the N-tail of cTnT to overlapping Tm while orienting the rest of cTn to actin. A 30 ps simulation was performed at cryogenic temperatures while the NOE constraints were gradually reduced to zero. The resulting structure successfully reached thermodynamic equilibrium as shown in Figure 3 and was allowed to evolve for 50 ps. We validated this low-temperature model by subtracting equilibrium atom–atom distances of our model from atom–atom distances of the structural sources. The results, shown in Figure 4, prove that our low-temperature dynamic model is faithful to its separate structural sources. We used this low-temperature structure as a common starting structure for simulations at physiologic temperature.

We took two thin filament models at low temperatures and removed a calcium ion from site II of cTnC from one of them. The two models were then subjected to identical minimization, heating, and equilibration conditions. They were minimized by alternating the SD and ABNR methods until they were energy optimized (final gradient of <0.0001 kcal mol<sup>-1</sup> Å<sup>-1</sup>), and then the Berendsen thermostat was used to gradually heat the

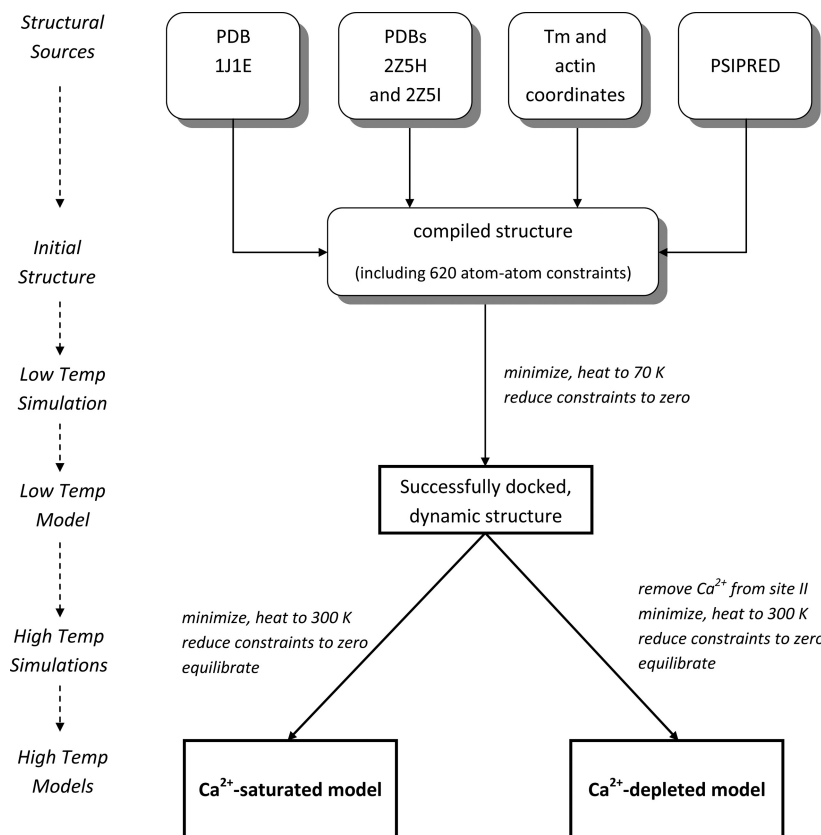


**Figure 2.** Schematic of the building and simulation processes of our model.

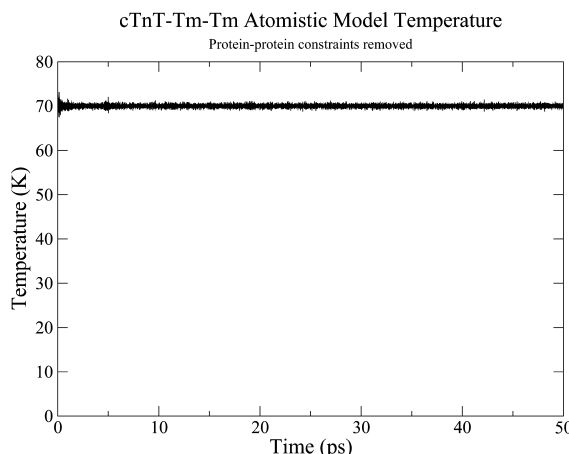


**Figure 3.** Temperature monitoring for 50 ps equilibration of the docked cTn-Tm complex.

systems from 0 to 300 K over 30 ps. When the temperature reached 300 K, nonoverlapping regions of tropomyosin were constrained in their closed state positions while the overlapping region of Tm was allowed to move freely; harmonic force constraints of 2 kcal mol<sup>-1</sup> Å<sup>-2</sup> were placed on C<sub>α</sub> atoms of residues 205 and 277 of cTnT, while the remainder of cTn was allowed to move freely. The system was again allowed to equilibrate for 30 ps in this free state. The system then evolved for 1 ns.

We recognize that 1 ns simulations will seem relatively short to the general population; however, 1 ns simulations of a system this size are at the limit of current computational

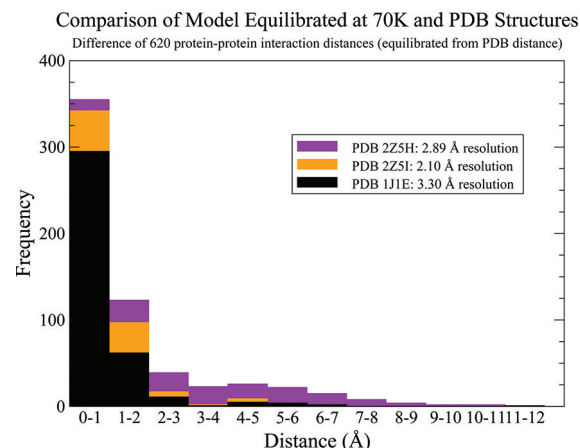


**Figure 4.** Histogram of the absolute values of equilibrated atom-atom distances subtracted from PDB atom-atom distances to demonstrate the validity of the model.

possibilities and preclude its explicit solvation. It has been shown that multiple short simulations are more likely indicative of molecular behavior than a single long simulation;<sup>30</sup> therefore, we ran 12 separate simulations with random initial conditions, six with and six without calcium in site II. We show the results of one below, but we report that qualitatively all results are the same for the remaining simulations.

This provided us with equilibrium MD simulations of the entire cTn-overlapping Tm complex virtually free of constraints whose starting structures differed only by a single atom, a Ca<sup>2+</sup> ion in site II of cTnC. These represent our

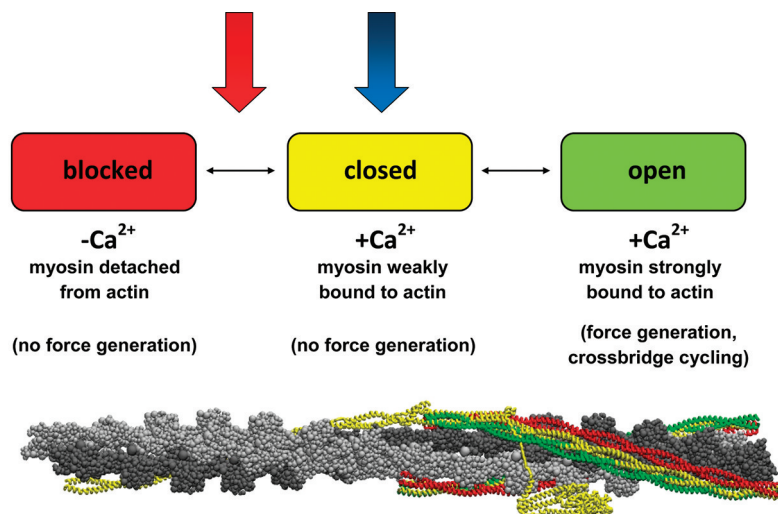


**Figure 5.** Tm explores three states of equilibrium (blocked, closed, and open), while the cTn core remains relatively stationary with respect to actin.<sup>10</sup> This system is in constant flux among the three equilibrium positions of Tm, where the length of an entire cardiac contraction cycle involving all three of these states is on the order of 100 ms.<sup>15</sup> We investigate how calcium directly affects the regulatory proteins cTn and Tm by looking at two representative equilibrium states with 1 ns simulations in the closed state and a position between the closed and blocked states and by comparing the changes between them. These two states are represented by the blue and red arrows, representing the Ca<sup>2+</sup>-saturated and Ca<sup>2+</sup>-depleted states, respectively.

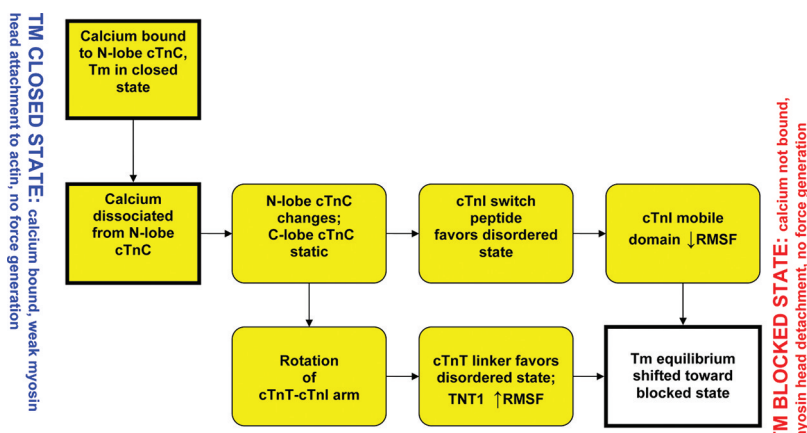


**Figure 6.** Schematic of the two-prong mechanism of Ca<sup>2+</sup> activation of the thin filament via regulatory proteins. The mechanistic changes captured by our model are highlighted in yellow.

calcium-saturated and calcium-depleted state models at physiologic temperature. Figure 5 identifies where these two models fall within the three-state model. The calcium-saturated model is the thin filament in the closed state; the calcium-depleted model is the thin filament without calcium bound between the closed and blocked states. Our calcium-depleted model is not entirely in the blocked state because the nonoverlapping tropomyosin remains fixed in the closed state.

The simulations were visualized with VMD.<sup>24</sup> Root-mean-square fluctuation (rmsf), hydrogen bond (cutoff of 2.4 Å), and root-mean-square deviation (rmsd) analyses were performed using CHARMM version 33b1.<sup>22,23</sup> Only the backbone atoms (amine N, C<sub>α</sub>, and carboxyl C) were used in calculating rmsf and rmsd. Secondary structure analyses were performed with STRIDE.<sup>25</sup> Contact maps were constructed using SPACE.<sup>26</sup>

**Statistical Methods.** The nature of proteins and protein dynamics presents unique challenges in analysis of their data. The data from these simulations are complex multivariate data clearly correlated by the nature of their peptide bonds as well as

their secondary, tertiary, and quaternary structure interactions. Both rmsf and hydrogen bond data appear to follow a gamma distribution pattern. There does not appear to be a standard statistical technique for addressing the analysis of our data because it is nonlinear, highly correlated, and non-Gaussian in nature. Because of this, the method of generalized estimating equations (GEE) appears to be a good choice for comparing Ca<sup>2+</sup>-saturated and Ca<sup>2+</sup>-depleted data. GEE is a general method for analyzing longitudinal data that is correlated.<sup>27</sup> A gamma model was fit with an inverse link function using an independent working correlation matrix with the robust sandwich variance estimator.<sup>28,29</sup> Statistical analyses were conducted with the software package R 2.11.1 for Windows. The test statistic used with GEE in R is the Wald test statistic.<sup>29</sup>  $p < 0.05$  is defined as being statistically significant.

## RESULTS AND DISCUSSION

Files containing three-dimensional structural information for the cTn–Tm complex in the Ca<sup>2+</sup>-saturated state at low

temperatures,  $\text{Ca}^{2+}$ -saturated state at physiologic temperature, and  $\text{Ca}^{2+}$ -depleted state at physiologic temperature are available in PDB format. Movies of the 1 ns simulations at 300 K in the  $\text{Ca}^{2+}$ -saturated and  $\text{Ca}^{2+}$ -depleted states prepared in VMD are available in Moving Picture Expert Group (.mpg) format. Similarly prepared movies of the switch peptide of cTnI interacting with the N-lobe of cTnC in the  $\text{Ca}^{2+}$ -saturated and  $\text{Ca}^{2+}$ -depleted states are also available.

**Low-Temperature Simulation.** The results of our low-temperature simulation show that it is possible to create a complete, dynamic model from multiple structural models. The temperature of the system for the 50 ps equilibration phase of the low-temperature simulation, shown in Figure 3, demonstrates that the system is in thermodynamic equilibrium. The rmsd over the course of equilibration decreased from 8 Å to a constant of  $\sim 1$  Å. The cTnT–Tm NOE constraints effectively docked TNT1, an N-terminal domain of cTnT, to the overlapping Tm with a high degree of similarity to the distance constraints detailed by PDB entries 2ZSH and 2ZSI, as shown in Figure 4. With all NOE constraints removed, 81% of the 620 dynamic protein–protein interactions differ by less than 4 Å from the static structural solutions. The resolution of the various crystal structures against which these equilibrated, dynamic distances are being compared ranges from 2.10 to 3.30 Å. The majority of differences fall within the range of 0–2 Å, reflecting a high degree of fidelity. The overall structure of our model displays an appearance similar to that of recent experimental results, including the close association of the N-tail of cTnT with Tm.<sup>31</sup>

**Physiologic-Temperature Simulations.** We observe two major routes by which cTn dynamics are able to shift the Tm equilibrium toward the closed state as a result of the removal of a calcium ion from site II of cTnC, summarized in Figure 6. First, the known, direct interactions of the N-lobe of cTnC with the switch peptide of cTnI causes fluctuations of the inhibitory and mobile domains of cTnI favoring the shift in the Tm equilibrium toward the blocked state.<sup>32,33</sup> Second, the changes in the N-lobe of cTnC alter the apex of the I-T arm, while interactions between the static C-lobe of cTnC and the cTn–actin species stabilize the base of the I-T arm, thus causing a rotation of the I-T arm. These changes in the I-T arm propagate downstream through the cTnT linker to overlapping Tm via the cTnT–Tm interactions, ultimately causing significant changes in overlapping Tm.

The rmsd values over the course of the 1 ns simulations were stable at 5 Å for both  $\text{Ca}^{2+}$ -saturated and  $\text{Ca}^{2+}$ -depleted states. Figure 7 shows areas in which subtle changes in structure are seen in our model as a function of calcium binding: the N-lobe of cTnT sites I and II and the linker between them; the switch peptide, the vicinity of residue 25, and the mobile domain of cTnI; and the linker and Tm-binding regions of cTnT (shown in RMSF analyses for cTn subunits and subsets, Secondary structure analysis, and Contact maps of the Supporting Information). The calcium-dependent changes apparent in Figure 7 are more easily visualized with structural images. Average structures of each model, calcium-saturated (blue) and calcium-depleted (red), are shown in Figure 8. Figure 8 identifies key structural regions that are important for the propagation of calcium signaling through the thin filament. (1) Changes in the N-lobe of cTnC directly alter the switch peptide and surrounding domains of cTnI. (2) Changes in the N-lobe of cTnC cause a rotation of the I-T arm, which relays the signal

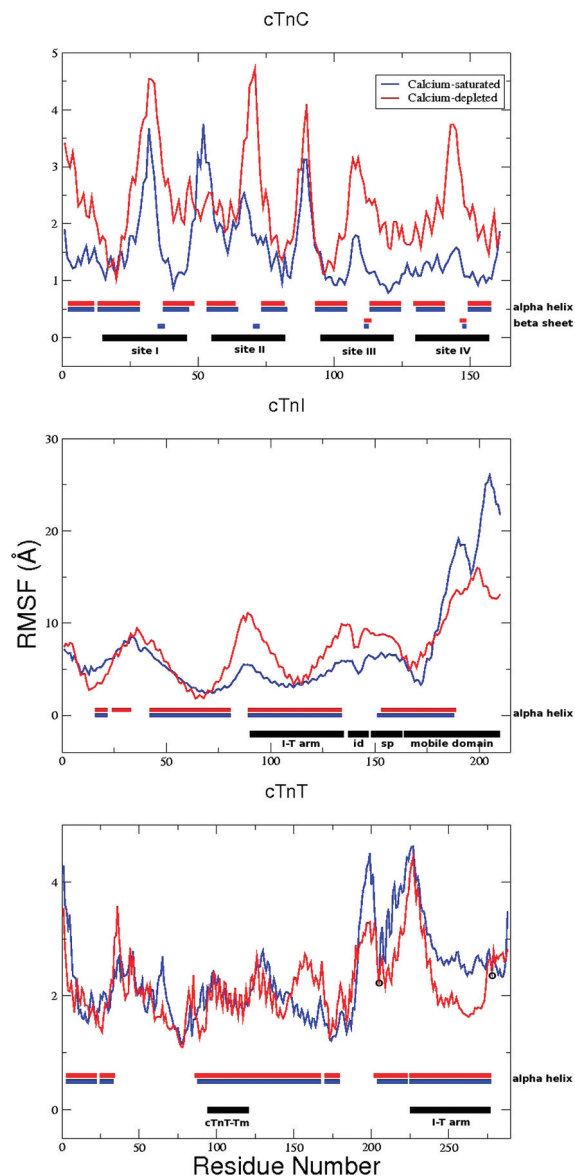


**Figure 7.** rmsf analysis for 1 ns simulations: (top) cTnC, (middle) cTnI, and (bottom) cTnT. Regions of structural and functional interest are identified in black horizontally along the bottom of each graph. Average secondary structure is identified horizontally along the bottom of each graph where structured residues are blocked, blue for  $\text{Ca}^{2+}$ -saturated and red for  $\text{Ca}^{2+}$ -depleted, and unstructured residues are left blank. cTnI and cTnT secondary structure consists solely of  $\alpha$ -helices (blocked) and coils (blank). id denotes the inhibitory domain and sp the switch peptide. Black circles represent constraints on  $C_{\alpha}$  atoms 205 and 277 of cTnT; all other atoms are allowed to move freely.

downstream through the cTnT linker to overlapping Tm (connections between Figures 7 and 8 are shown in RMSF and structural correspondence in the Supporting Information).

**cTnC–cTnI Interactions Are Altered as a Function of  $\text{Ca}^{2+}$  Binding.** The N-lobe of cTnC undergoes significant change when  $\text{Ca}^{2+}$  is removed from site II, but the C-lobe does not as shown in Figure 9. Our results match existing solution structures of calcium-depleted and calcium-saturated cTnC, including regions of  $\alpha$ -helices,  $\beta$ -sheets, and less well-defined regions that correspond to regions with an increased rmsf in

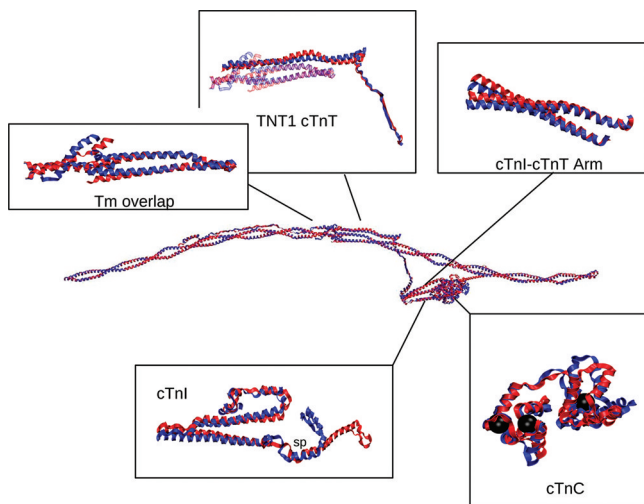


**Figure 8.** Alignment of  $\text{Ca}^{2+}$ -saturated and  $\text{Ca}^{2+}$ -depleted average structures of the complete cTn complex with overlapping Tm and highlighted regions of interest. The color scheme for this and the other structural images is as follows: blue for  $\text{Ca}^{2+}$ -saturated and red for  $\text{Ca}^{2+}$ -depleted. In cTnC, the black spheres represent the locations of calcium ions. In the cTnI box, sp denotes the switch peptide.

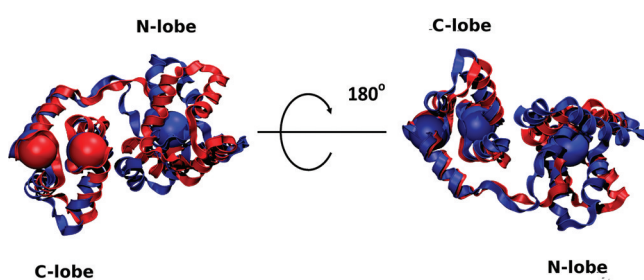


**Figure 9.** Alignment of  $\text{Ca}^{2+}$ -saturated and  $\text{Ca}^{2+}$ -depleted average structures of cTnC. Calcium ion locations are shown as large spheres colored according to their appropriate state. Note the lack of a calcium ion in the N-lobe in the  $\text{Ca}^{2+}$ -depleted state. There is significant change in the conformation of the N-lobe, while the C-lobe remains mostly unchanged. The  $\text{Ca}^{2+}$  ion positions bound to the C-lobe in the two states are virtually superimposed. Binding sites I and II as well as the linker between them are significantly altered as a result of the removal of  $\text{Ca}^{2+}$ . This corresponds to the changes in rmsf that we see in Figure 7.

our results [such as the N- and C-terminal residues, sites I (residues 30–34) and II (residues 65–70), the B–C linker (residues 49–53), and the central linker (residues 84–93), as shown in Figure 7].<sup>34,35</sup> We also observe an increase in the number of fluctuations in sites I and II in the calcium-depleted state, which results in them being less well-defined. This is in direct agreement with NMR observations.<sup>34</sup> These results are reflected in all of our calcium-saturated and -depleted simulations.

The switch peptide of cTnI and its surrounding regions, the inhibitory and mobile domains, are significantly affected by changes in the N-lobe of cTnC. Our results concur with the “fly-cast” mechanism by which alterations in the switch peptide translate its alternating order and disorder into the altered dynamics of nearby regions.<sup>32,33,36</sup> We see stronger folding occur in the switch peptide in the  $\text{Ca}^{2+}$ -saturated state, allowing this hydrophobically rich region of cTnI to differ-

entially interact with the N-lobe of cTnC, visually demonstrated in the movies. As a result, the nearby inhibitory and mobile domains are less likely to interact with actin, allowing Tm to more easily shift to the open state.

The  $\text{Ca}^{2+}$ -depleted behavior of the mobile domain of cTnI shown in Figure 10, however, shifts the equilibrium of Tm

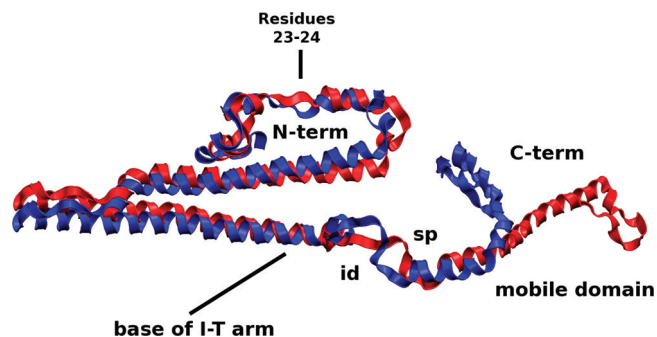


**Figure 10.** Alignment of  $\text{Ca}^{2+}$ -saturated and  $\text{Ca}^{2+}$ -depleted average structures of cTnI. The N-terminus and switch peptide and surrounding regions of the C-terminus interact with the N-lobe of cTnC and are altered as a function of  $\text{Ca}^{2+}$  binding. As a result, fluctuations in the dynamics of the N-lobe cTnC alter the dynamics of the switch peptide of the C-terminus of cTnI and the N-terminus of cTnI. id denotes the inhibitory domain and sp the switch peptide.

toward the blocked position. The decreased rmsf of the mobile domain in the  $\text{Ca}^{2+}$ -depleted suggests it is more rigid, a finding that is experimentally confirmed.<sup>33</sup> This is clearly seen in the movies of the simulation (see the Supporting Information); it is the single greatest change observed when visually comparing the two simulations. In approximately 500 ps, the mobile domain of cTnI in the  $\text{Ca}^{2+}$ -depleted state “reaches out” toward Tm and binds to it. The rigid nature of the mobile domain of cTnI in the  $\text{Ca}^{2+}$ -depleted state puts it in a more advantageous position to interact with Tm or actin and sterically blocks Tm more toward the states of equilibrium farthest from the cTn core, which as shown in Figure 5 are the closed and blocked states. The mobile domain in the  $\text{Ca}^{2+}$ -saturated state is far more flexible as shown in Figure 7 and the movies, findings that are also experimentally confirmed,<sup>33</sup> which would allow Tm to maximally explore equilibrium states near and far from the cTn core, i.e., open, closed, or blocked states. These results were qualitatively the same for all of our calcium-saturated and -depleted simulations. A recent experiment demonstrated findings similar to our simulations, namely that the C-terminal of TnI, residues 157–163, interacted with Tm residue 146 in the absence of  $\text{Ca}^{2+}$ .<sup>37</sup> In our model, cTnI in the vicinity of residues 190–195 is capable of interacting with C-terminal Tm in the vicinity of residue 120 only in the  $\text{Ca}^{2+}$ -depleted state. More recently, it was shown that the last 17 residues of cTnI stabilize Tm in the closed state.<sup>5</sup> Our simulations show the same region of cTnI interacting with Tm in the closed state position.

#### $\text{Ca}^{2+}$ -Dependent Changes in the N-Terminus of cTnI.

We also see the N-terminal region of cTnI affected by the calcium-dependent change in the N-lobe of cTnC, which results in a rotation of the I-T arm shown in Figure 11. The “apex” of the I-T arm is directly affected by the mobility of the N-terminus of cTnI, while the “base” of the I-T arm is stabilized by the C-lobe of cTnC. We found through hydrogen bond

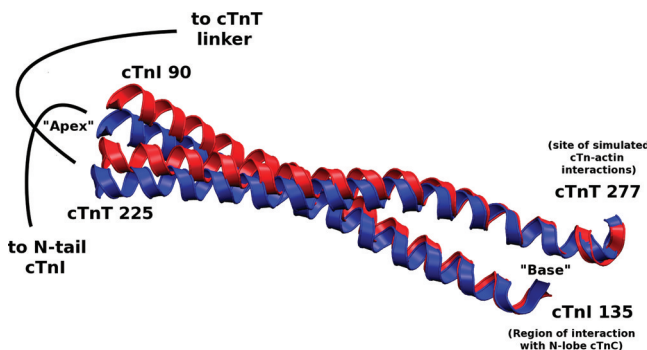


**Figure 11.** Alignment of  $\text{Ca}^{2+}$ -saturated and  $\text{Ca}^{2+}$ -depleted average structures of the cTnI–cTnT coiled coil (I-T arm). This is the most stable region of the entire complex (in terms of subunit–subunit interactions), allowing the I-T arm to behave as a united pair. The stable portion of the arm (in terms of dynamics) is at the base of the arm, which is where cTnI interacts with the C-lobe of cTnC and where cTnT is simulated to interact with actin. The stable base allows the apex of the I-T arm to rotate because of fluctuations in the N-terminus of cTnI. The I-T arm rotation causes fluctuations in the cTnT linker.

analysis that the I-T arm is the most stable region of the complex in terms of subunit–subunit interactions. This concurs with recent experimental findings using hydrogen–deuterium exchange<sup>6</sup> (see Hydrogen bond analysis in the Supporting Information). The stable nature of the I-T arm makes it function like a rigid rod capable of moving as a single unit. While the N-terminus of cTnI causes the apex of the I-T arm to move, the base is relatively fixed because of interactions with the C-lobe of cTnC and cTn–actin interactions. The average position of the I-T arm differs by an rmsd of 1.2 Å and a rotation of 5° between the coiled coils shown in Figure 11. This confirms speculation that a small rotation occurs about a pivot point at the C-terminus of the I-T arm.<sup>7</sup> Because of the I-T arm's stable base, its helical components appear to rotate about one another at the apex. We also observe significant changes in the position and dynamic behavior of residues 23 and 24 of cTnI, the cardiac specific phosphorylation sites responsible for the inotropic effects of  $\beta$ -adrenergic agonists,<sup>38,39</sup> as a function of  $\text{Ca}^{2+}$  binding. We observe significant change in the mobility of the protein complex at the phosphorylation sites in the calcium-saturated and -depleted models even though the average secondary structure is not greatly effected by calcium binding. Thus, dynamic properties cannot be inferred from static structures and are rather dependent upon interactions throughout the complex. These results are qualitatively similar for all calcium-saturated and -depleted simulations.

This brings to light a plausible mechanism in atomic detail by which the cTnT linker region, residues 170–204 of cTnT, may act to propagate calcium signaling; it is a dynamic filter fine-tuned to calcium binding. This means it functionally connects the C-terminal (core) and N-terminal (Tm binding) domains of cTnT.

**Dual Functionality of cTnT.** Significant changes in the I-T arm are transduced to Tm via the cTnT linker, which connects the I-T arm to overlapping Tm, shown in Figure 12. This observation helps to explain the underlying reason why early experimental results showed that the cTnT C-terminus was necessary for cTnT–cTnI–cTnC  $\text{Ca}^{2+}$ -sensitive interactions,<sup>40</sup> while the N-tail of cTnT is required for cooperative activation of the thin filament.<sup>41</sup> The cTnT linker physically and

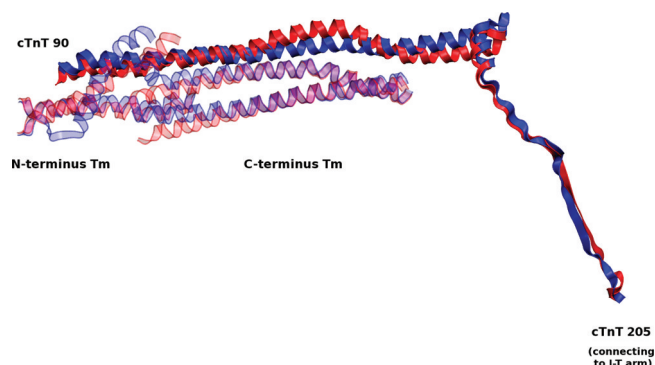


**Figure 12.** Alignment of  $\text{Ca}^{2+}$ -saturated and  $\text{Ca}^{2+}$ -depleted average structures of the cTnT linker. Fluctuations from the apex of the I-T arm are passed through the cTnT linker to overlapping Tm.

functionally connects the two distinct roles of cTnT's N- and C-tail domains, as was hypothesized by recent experimental findings.<sup>42</sup> Here we see it demonstrated in a dynamic model with atomic detail. The importance of this region is underscored by the evolutionary conservation of its primary sequence and the lack of disease-causing mutations.<sup>7,43</sup>

The cTnT linker, in a final step of signal transduction, relays fluctuations to the TNT1 region of cTnT, which is directly bound to overlapping Tm (Figures 7 and 12). Unfolding occurs in the linker region, residues 170–204, in the  $\text{Ca}^{2+}$ -depleted state. As a result, the region distant from the core, residues 150–170, swings relatively freely, perturbing Tm equilibrium. The region of cTnT–Tm binding is relatively stable, allowing the cTnT–Tm complex to move as a single unit, reminiscent of the I-T arm. This is confirmed by early experimental studies demonstrating the  $\text{Ca}^{2+}$ -insensitive nature of cTnT–Tm binding in this region;<sup>44</sup> here, we observe it in a complete dynamic model. Gordon notes that in this position, cTnT is “in a position to influence the flexibility of Tm, since the Tm overlap region is responsible for much of the affinity of Tm for actin and Tm shows its greatest flexibility in this region.”<sup>15</sup> Biophysical studies have suggested the importance of stability in this crucial region and the dysfunction caused by mutations here because of alterations in flexibility.<sup>8</sup> Simulations of protein segments in this region by our laboratories have demonstrated physical mechanisms by which these mutants act, specifically changes in bending forces as a result of hot spot mutations.<sup>1,2</sup> Despite the relatively small region of freely moving Tm in our model, we notice significant changes in the overlapping Tm. A loss of secondary structure in Tm at the junction between constrained and free Tm is visually observed between the  $\text{Ca}^{2+}$ -saturated and  $\text{Ca}^{2+}$ -depleted states, as seen in Figure 13. This net structural change is a reflection of differential forces transmitted through the cTn complex as a function of  $\text{Ca}^{2+}$  binding. These significant dynamic changes in overlapping Tm, coupled to the fact that Tm bends anisotropically,<sup>11</sup> support the idea that these small variations in overlapping Tm dynamics induced by cTn may be sufficient to perturb Tm dynamics toward a new equilibrium, favoring either a blocked or open state.<sup>9</sup>

Because our model is capable of capturing changes only in overlapping Tm, we cannot observe the entire shift in the equilibrium state of the entire set of strands. While we cannot say definitively that the Tm would shift to the blocked state rather than the open state because of these changes, on the

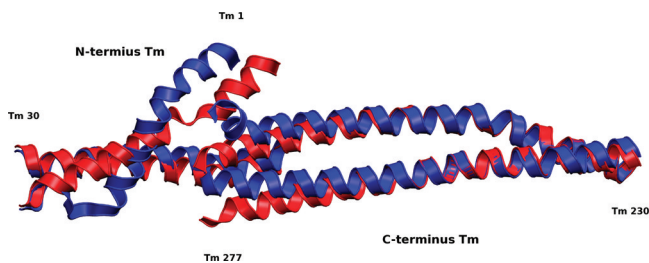


**Figure 13.** Alignment of  $\text{Ca}^{2+}$ -saturated and  $\text{Ca}^{2+}$ -depleted average structures of overlapping Tm. The overlapping region of Tm is important for its affinity for actin and flexibility.<sup>15</sup> The significant changes we observe in this region appear despite the fact that both strands of Tm are constrained at each end by the remaining Tm in the closed position. The loss of secondary structure we observe in these average structures is likely the result of resistance to fluctuations by these constraints, an indicator that changes in this region could shift the equilibrium of more than just the overlap region. We expect that the loss of secondary structure would not occur if the remainder of Tm was allowed to move freely and that Tm would shift toward the blocked state when our model is in the  $\text{Ca}^{2+}$ -depleted state, and possibly toward the open state when our model is in the  $\text{Ca}^{2+}$ -saturated state, which would work in tandem with actomyosin interactions. In our model, residues 245–277 of the C-terminus of Tm and residues 1–30 of the N-terminus of Tm are allowed to move freely, and the remaining residues have their  $\alpha$ -carbons fixed in the closed position.

basis of the overwhelming agreement between our results and experimental findings, it is relatively safe to assume that the changes we observe in overlapping Tm as a result of the removal of a calcium ion from site II of cTnC would assist in the shift of the entire set of strands of Tm toward the blocked state rather than to the open state.

## CONCLUSION

We have presented a dynamic model of the thin filament compiled from existing structures and models of cardiac troponin, tropomyosin, and actin that it is capable of replicating key experimental findings with atomic detail. Through molecular dynamics simulations, we were able to find that small changes in structure and protein contacts within cardiac troponin result in large changes throughout the complex. These cTn changes affect tropomyosin dynamics and cardiac troponin–actin interactions. The minor changes in structure as a function of calcium binding we saw were as follows: the N-lobe of cTnT sites I and II and the linker between them; the switch peptide, the vicinity of residues 20–25, and the mobile domain of cTnI; and the linker region and N-tail of cTnT. The large changes in the dynamics we saw were as follows: the mobile domain of cTnI, the I-T arm, the cTnT linker, and overlapping Tm. Our model demonstrates a comprehensive mechanism for calcium activation of the cardiac thin filament validated by experimental findings.

## ASSOCIATED CONTENT

### Supporting Information

Primary sequence alignment, secondary structure, compilation of known and predicted structures of the cTn complex, compilation of known structures of overlapping Tm, protein–protein interactions, Tm–Tm overlap, Tm–TnT interactions, hcTnT substitution of *Gallus gallus* fsTnT-specific interactions, orientation of cTn over actin, cTn simulations without Tm,

rmsf analyses for cTn subunits and subsets, secondary structure analysis, contact maps, rmsf and structural correspondence, and hydrogen bond analysis. This material is available free of charge via the Internet at <http://pubs.acs.org>.

## AUTHOR INFORMATION

### Corresponding Author

\*E-mail: sschwartz@aecon.yu.edu. Phone: (718) 430-2139. Fax: (718) 430-8819.

### Funding

This work has been supported in part by National Institutes of Health (NIH) Grant HL075619 (to J.C.T.), NIH Grant GM068036 (to S.D.S.), and NIH Grant HL107046-01 (to J.C.T. and S.D.S.).

## ABBREVIATIONS

cTn, cardiac troponin; cTnC, cardiac troponin C; cTnT, cardiac troponin T; cTnI, cardiac troponin I; Tm, tropomyosin.

## REFERENCES

- (1) Ertz-Berger, B., He, H., Dowell, C., Factor, S., Haim, T., Nunez, S., Schwartz, S. D., Ingwall, J., and Tardiff, J. (2005) Changes in the chemical and dynamic properties of cardiac troponin T cause discrete cardiomyopathies in transgenic mice. *Proc. Natl. Acad. Sci. U.S.A.* **102**, 18219–18224.
- (2) Guinto, P. J., Manning, E. P., Schwartz, S. D., and Tardiff, J. C. (2007) Computational characterization of mutations in cardiac troponin T known to cause familial hypertrophic cardiomyopathy. *J. Theor. Comput. Chem.* **6**, 413–419.
- (3) Kobayashi, T., and Solaro, R. J. (2005) Calcium, Thin Filaments, and the Integrative Biology of Cardiac Contractility. *Annu. Rev. Physiol.* **67**, 39–67.
- (4) Tobacman, L. S. (1996) Thin filament-mediated regulation of cardiac contraction. *Annu. Rev. Physiol.* **58**, 447–481.
- (5) Galinska, A., Hatch, V., Craig, R., Murphy, A. M., Eyk, J. E. V., Wang, C.-L. A., Lehman, W., and Foster, D. B. (2010) The C Terminus of Cardiac Troponin I Stabilizes the  $\text{Ca}^{2+}$ -Activated State of Tropomyosin on Actin Filaments. *Circ. Res.* **106**, 705–711.
- (6) Kowlessur, D., and Tobacman, L. S. (2010) Troponin Regulatory Function and Dynamics Revealed by H/D Exchange-Mass Spectrometry. *J. Biol. Chem.* **285**, 2686–2694.
- (7) Takeda, S., Yamashita, A., Maeda, K., and Maeda, Y. (2003) Structure of the core domain of human cardiac troponin in the  $\text{Ca}^{2+}$ -saturated form. *Nature* **424**, 35–41.
- (8) Palm, T., Graboski, S., Hitchcock-DeGregori, S.E., and Greenfield, N.J. (2001) Disease-causing mutations in cardiac troponin T: Identification of a critical tropomyosin-binding region. *Biophys. J.* **81**, 2827–2837.
- (9) Murakami, K., Stewart, M., Nozawa, K., Tomii, K., Kudou, N., Igarashi, N., Shirakihara, Y., Wakatsuki, S., Yasunaga, T., and Wakabayashi, T. (2008) Structural basis for tropomyosin overlap in thin (actin) filaments and the generation of a molecular swivel by troponin-T. *Proc. Natl. Acad. Sci. U.S.A.* **105**, 7200–7205.
- (10) Pirani, A., Vinogradova, M. V., Curni, P. M. G., King, W. A., Fletterick, R. J., Craig, R., Tobacman, L. S., Xu, C., Hatch, V., and Lehman, W. (2006) An Atomic Model of the Thin Filament in the Relaxed and  $\text{Ca}^{2+}$ -Activated States. *J. Mol. Biol.* **357**, 707–717.
- (11) Li, X., Holmes, K. C., Lehman, W., Jung, H. S., and Fischer, S. (2010) The Shape and Flexibility of Tropomyosin Coiled Coils: Implications for Actin Filament Assembly and Regulation. *J. Mol. Biol.* **395**, 327–339.
- (12) Poole, K. J. V., Lorenz, M., Evans, G., Rosenbaum, G., Pirani, A., Craig, R., Tobacman, L. S., Lehman, W., and Holmes, K. C. (2006) A comparison of muscle thin filament models obtained from electron

- microscopy reconstructions and low-angle X-ray fiber diagrams from non-overlap muscle. *J. Struct. Biol.* 155, 273–284.
- (13) McKillop, D.F. A., and Geeves, M. A. (1993) Regulation of the Interaction between Actin and Myosin Subfragment 1: Evidence for Three States of the Thin Filament. *Biophys. J.* 65, 693–701.
- (14) Gordon, G. M., Hamsher, E., and Regnier, M. (2001) Skeletal and Cardiac Muscle Contractile Activation: Tropomyosin “Rocks and Rolls”. *News Physiol. Sci.* 16, 49–55.
- (15) Gordon, A. M., Hamsher, E., and Regnier, M. (2000) Regulation of Contraction in Striated Muscle. *Physiol. Rev.* 80, 853–924.
- (16) <http://www.mpimf-heidelberg.mpg.de/holmes>, accessed March 24, 2009.
- (17) <ftp://149.217.48.3/pub/holmes>, accessed March 24, 2009.
- (18) Bryson, K., McGuffin, L. J., Marsden, R. L., Ward, J. J., Ward, J. S., Sodhi, J. S., and Jones, D. T. (2005) Protein structure prediction servers at University College London. *Nucleic Acids Res.* 33, W36–W38.
- (19) Jones, D. T. (1999) Protein secondary structure prediction based on position-specific scoring matrices. *J. Mol. Biol.* 292, 195–202.
- (20) Vinogradova, M. V., Stone, D. B., Malanina, G. G., Karatzafiri, C., and Cooke, R. (2005)  $\text{Ca}^{2+}$ -regulated structural changes in troponin. *Proc. Natl. Acad. Sci. U.S.A.* 102, 5038–5043.
- (21) Laskowski, R. A. (2009) PDBsum new things. *Nucleic Acids Res.* 37, D355–D359.
- (22) Brooks, B. R., et al. (2009) CHARMM: The biomolecular simulation program. *J. Comput. Chem.* 30, 1545–1614.
- (23) Brooks, B. R., Bruccoleri, R. E., Olafson, B. D., States, D. J., Swaminathan, S., and Karplus, M. (1983) CHARMM: A program for macromolecular energy, minimization, and dynamics calculations. *J. Comput. Chem.* 4, 187–217.
- (24) Humphrey, W., Dalke, A., and Schulten, K. (1996) VMD: Visual Molecular Dynamics. *J. Mol. Graphics* 14, 33–38.
- (25) Heinig, M., and Frishman, D. (2004) STRIDE: A web server for secondary structure assignment from known atomic coordinates of proteins. *Nucleic Acids Res.* 32, W500–W502.
- (26) Sobolev, V., Eyal, E., Gerzon, S., Potapov, V., Babor, M., Prilusky, J., and Edelman, M. (2005) SPACE: A suite of tools for protein structure prediction and analysis based on complementarity and environment. *Nucleic Acids Res.* 33, W39–W43.
- (27) Diggle, P. J., Liang, K.-Y., and Zeger, S. L. (1996) *Analysis of Longitudinal Data*, Oxford University Press, Oxford, U.K.
- (28) Hanley, J. A., Negassa, A., Edwardes, M. D., and Forrester, J. E. (2003) Statistical Analysis of Correlated Data Using Generalized Estimating Equations: An Orientation. *Am. J. Epidemiol.* 157, 364–375.
- (29) Halekoh, U., Hojsgaard, S., and Yan, J. (2006) The R Package geepack for Generalized Estimating Equations. *J. Stat. Software* 15, 1–11.
- (30) Caves, L. S., Evanseck, J. D., and Karplus, M. (1998) Locally accessible conformations of proteins: Multiple molecular dynamics simulations of crambin. *Protein Sci.* 7, 649–666.
- (31) Paul, D. M., Morris, E. P., Kensler, R. W., and Squire, J. M. (2009) Structure and Orientation of Troponin in the Thin Filament. *J. Biol. Chem.* 284, 15007–15015.
- (32) Hoffman, R. M. B., and Sykes, B. D. (2008) Isoform-specific variation in the intrinsic disorder of troponin I. *Proteins* 73, 338–350.
- (33) Hoffman, R. M. B., Blumenschein, T. M. A., and Sykes, B. D. (2006) An Interplay between Protein Disorder and Structure Confers the  $\text{Ca}^{2+}$  Regulation of Striated Muscle. *J. Mol. Biol.* 361, 625–633.
- (34) Spyropoulos, L., Li, M. X., Sia, S. K., Gagne, S. M., Chandra, M., Solaro, R. J., and Sykes, B. D. (1997) Calcium-induced structural transition in the regulatory domain of human cardiac troponin C. *Biochemistry* 36, 12138–12146.
- (35) Sia, S. K., Li, M. X., Spyropoulos, L., Gagne, S. M., Liu, W., Putkey, J. A., and Sykes, B. D. (1997) Structure of cardiac muscle troponin C unexpectedly reveals a closed regulatory domain. *J. Biol. Chem.* 29, 18216–18221.
- (36) Shoemaker, B. A., Portman, J. J., and Wolynes, P. G. (2000) Speeding molecular recognition by using the folding funnel: The fly-casting mechanism. *Proc. Natl. Acad. Sci. U.S.A.* 97, 8868–8873.
- (37) Mudalige, W. A. K. A., Tao, T. C., and Lehrer, S. S. (2009)  $\text{Ca}^{2+}$ -Dependent Photocrosslinking of Tropomyosin Residue 146 to Residues 157–163 in the C-Terminal Domain of Troponin I in Reconstituted Skeletal Muscle Thin Filaments. *J. Mol. Biol.* 389, 575–583.
- (38) Solaro, R. J., Moir, A. J. G., and Perry, S. V. (1976) Phosphorylation of troponin I and the inotropic effect of adrenaline in the perfused rabbit heart. *Nature* 262, 615–617.
- (39) Mittmann, K., Jaquet, K., and Heilmeyer, L. M. B. (1990) A common motif of two adjacent phosphoserines in bovine, rabbit and human cardiac troponin I. *FEBS Lett.* 273, 41–45.
- (40) Pearlstone, J. R., and Smillie, L. B. (1983) Effects of Troponin-I Plus-C on the Binding of Troponin-T and Its Fragments to  $\alpha$ -Tropomyosin. *J. Biol. Chem.* 258, 2534–2542.
- (41) Schaertl, S., Lehrer, S. S., and Geeves, M. A. (1995) Separation and characterization of the two functional regions of troponin involved in muscle thin filament regulation. *Biochemistry* 34, 15890–15894.
- (42) Biesiadecski, B. J., Chong, S. M., Nosek, T. M., and Jin, J. P. (2007) Troponin T Core Structure and the Regulatory NH<sub>2</sub>-Terminal Variable Region. *Biochemistry* 46, 1368–1379.
- (43) Gomes, A. V., Barnes, J. A., Harada, K., and Potter, J. D. (2004) Role of troponin T in disease. *Mol. Cell. Biochem.* 263, 115–129.
- (44) Pearlstone, J. R., and Smillie, L. B. (1982) Binding of Troponin-T Fragments to Several Types of Tropomyosin. *J. Biol. Chem.* 257, 10587–10592.